

Original Research Article

# Advanced Control Techniques for Enhancing the Power System Stability at OOS Condition

Ali M. Eltamaly<sup>1\*</sup>, Yehia Sayed Mohamed<sup>2</sup>, Abou-Hashema M. El-Sayed<sup>2</sup>, Amer Nasr A. Elghaffar<sup>2\*\*</sup>

<sup>1</sup> Electrical Engineering Department, Mansoura University, Mansoura, Egypt

<sup>2</sup> Electrical Engineering Department, Minia University, Minia, Egypt

\* Corresponding Author: [eltamaly@ksu.edu.sa](mailto:eltamaly@ksu.edu.sa)

\*\* Corresponding Author: [amernasr70@yahoo.com](mailto:amernasr70@yahoo.com)

## ABSTRACT

The power system stability is the accurate operation of the electric grid by restoring balance after being subjected to an abnormal condition such as fault, line switching, load rejection, and loss of excitation. Protective equipment in high voltage substations should fast and precisely localize the faults. Some abnormal conditions in the power system such as out-of-step (OOS) condition which is not a real fault, but the protection equipment will consider it is. This misjudgment will cause the loss of synchronism between areas within the power system or between interconnected systems and will lead to blackout of the national grid. This paper studied the OOS condition, philosophy of protection relay device and how to avoid the false operation for distance function by Out of Step Blocking (OSB) by using the advanced protection relay, to improve the stability of power system.

**KEYWORDS:** Power System, OOS, Advanced Relay, Protection System and Transient.

Received: 18<sup>th</sup> Jan. 2019      Accepted: 6<sup>th</sup> Apr. 2019      Online: 20<sup>th</sup> Apr. 2019

## 1. Introduction

The power system quality is the main challenge at design the power system for saving the stable electric power source to the consumers. Stability in the power system is defined as the accurate operation of the system by recovering a state of operating balance after any abnormal condition such as faults, over or under voltage cases at switching time, load rejection and at loss of excitation<sup>[1]</sup>. Over Head Transmission Line (OHTL) is the main parts in the power system which transmits the power from the generation to the electrical loads<sup>[2]</sup>. OHTL is the most part that's face the faults in the system. So, it's important to use the protection system with OHTL, since, it's mostly extended across large geographical regions to transport the power from generators to load centers. So, it is possible to simulate faults along the OHTL which ranges from conduction that failure to loss of insulation<sup>[3]</sup>. Power Swing Condition (PSC) can be defined as a variation in three phase power equalized for voltage and also three phase current flow<sup>[4]</sup>. The power flow from generator to the grid is a high dynamic network connecting via OHTL. Figure 1 shows the single line diagram for the two sources power system, at stable conditions in power system, it is operated very compact to their nominal frequency (50 or 60 Hz) and typically maintain absolute voltage differences varies between 5%.

The frequency of a stable system varies between  $\pm 0.02$  Hz. The equalized in active power and reactive power between power generated and consumed exists during stable operating conditions<sup>[5]</sup>. The power flow in the power system, its effect

by any change or unstable in the loads or power generated, this change in power flow still in the network until reach to equalization between load demand and power generation<sup>[6]</sup>. These changes conditions in power flow happen more times, but it's immediately compensated by control systems, and normally have no detrimental effect on the power grid or its protective systems<sup>[7]</sup>. There are some abnormal conditions in power system, that's may lead to loss of synchronism between power generator and the rest of the utility system for the load, or between adjacent utility interconnected with power systems. At out of synchronism condition in power system, it is important to separate immediately the power generator or the system areas that's operating asynchronously, this separation to avoid widespread outages or lead to black out and equipment damage. An effective mitigating way to contain such a disturbance is done through control in the power system using the OOS function in protection systems. Researchers study OOS condition in power system by adjusting the Intelligent Electronic Devices (IEDs) to detect OOS by the time interval required by the apparent impedance locus to cross the two characteristics (buffer area), if the time exceeds a specified value, then the power swing blocking function is initiated<sup>[8]</sup>. But this method is not easily to simulate.

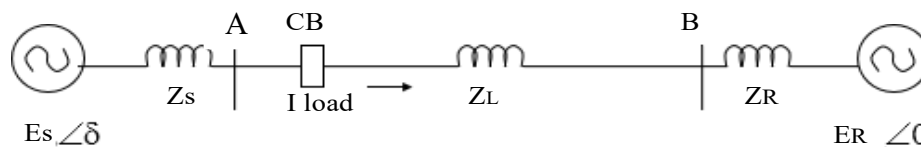


**Figure 1.** Single line diagram for two sources power system

#### Nomenclature

OOS	Out-Of-Step
OSB	Out-Of-Step Blocking
OST	Out-Of-Step Tripping
PSC	Power Swing Condition
EPS	Electrical Power System
IED	Intelligent Electronic Device
P	Active Power
$E_s$	Sending-end source voltage magnitude
$E_R$	Receiving-end source voltage magnitude
$\delta$	Angle difference between two sources
X	Total reactance of the transmission line
SLG	Single Line to Ground Fault
LL	Line to Line Faults
DLG	Double Line to Ground Faults
LLL	Three Phase Faults
OHTL	Over Head Transmission Line
-R - X	Arc of the circle
$\delta_1$	Rotor angle
tcr	Fault clearing time
H	The equivalent rotor angle inertia
ZL	The transmission line of impedance
$\delta_0$	Initial rotor angle

Also, may lead to false operation for OSB at some actions in power system such as starting inrush current. This inrush current generates at energizing the power transformer that's a one from loads for the OHL which need to design the OOS. So, this paper shows optimum design for distance protection function to control system by using IEDs that is achieved with an Out-Of-Step Blocking (OSB). However, OSB systems must be balanced with Out-Of-Step Tripping (OST) of distance relay elements or other IEDs functions to operate during unstable power swings. Using OSB by the design that shown in this paper will prevent the system black out or separate un-synchronizing area by false operation<sup>[9]</sup>.

## 2. Distance protection performance

Many years, the world has been successfully used for distance protection functions with OHTL<sup>[10]</sup>. It's considered the main protection for OHTL. The development in the protection relays from electromechanical relay and solid-state relays with mho quadrature to Intelligent Electronic Device (IEDs), numerical relay is the important factor in the widespread acceptance of this type of protection functions at different voltage levels all over the world<sup>[11]</sup>. The first zone in distance function protection is used to provide primary high-speed protection which operates instantaneous, to a significant portion of the transmission line. The second zone is used to cover the rest of the protected line and provide some backup for the remote end bus<sup>[10,11]</sup>. The third zone is the backup protection for the first and second zone for all the lines connected to the remote end bus. The applications for the distance function in IEDs are required for understanding of operating principles, with consideration the factors that effect on the performance of the protection relays under different abnormal conditions in power system<sup>[12]</sup>. The setting of distance IEDs should ensure that the relay is not going to operate when not required and will operate, only when it's necessary<sup>[10-12]</sup>. IEDs distance protection effectively measures the impedance between the relay location and the fault by measuring voltage and current in the transmission line. If the resistance of the fault is low, the impedance calculated is proportional to the distance from the current transformer which supplied the distance relay to the fault<sup>[13]</sup>. A distance protection function in IEDs is designed to protect the faults occurring in OHTL between the current transformer location, the selected reach point and remains stable for all faults outside this region or zones<sup>[14]</sup>.

## 3. Analysis of symmetrical fault in power system

To analyze the fault, it's important to simulate the fault in three components that's positive sequence and negative sequence and zero sequence. Figure 2a shows the positive sequence components are equal in magnitude values and the angle difference between each phase by 120 degrees with the same sequence as the original phases, also the currents and voltages follow the same cycle in typical counter clockwise rotation electrical system that's called the "abc". Figure 2b shows the negative sequence components that's equalized in magnitude, the phase shift between phases is 120° and its opposite phase sequence from the original system that's identified as "acb". Figure 4c shows the zero sequence components that's three-phase equalized in magnitude and the phase shift between phases is zero. The zero sequence components are not presented at symmetrical fault<sup>[15, 16]</sup>.

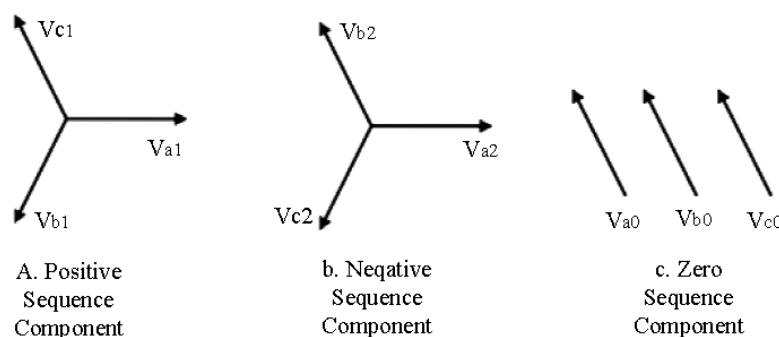


Figure 2. Analyze the sequence component in the power system

Firstly, the Change in magnitude:

$$a = 1 \angle 120^\circ = -0.5 + j0.866 \quad (1)$$

$$a^2 = 1 \angle 240^\circ = -0.5 - j0.866 \quad (2)$$

$$a^3 = 1 \angle 360^\circ = 1 + j0 \quad (3)$$

From these equations, useful combinations can be derived

$$1 + a + a^2 = 0$$

$$1 - a^2 = \sqrt{3} \angle 30^\circ \quad (4)$$

Or

$$1 - a = \sqrt{3} \angle -30^\circ$$

$$a^2 - a = \sqrt{3} \angle 270^\circ \quad (5)$$

Or

$$a - a^2 = \sqrt{3} \angle 90^\circ \quad (6)$$

Any three-phase system of phasors will always be the sum of the three components.

Positive sequence voltage is:

$$V_{a1} \quad V_{b1} \quad V_{c1}$$

Negative sequence voltage is:

$$V_{a2} \quad V_{b2} \quad V_{c2}$$

Zero sequence voltage is:

$$V_{a0} \quad V_{b0} \quad V_{c0}$$

The original system phase components can be presented from  $V_a$ ,  $V_b$  and  $V_c$ ,

$$V_a = V_{a0} + V_{a1} + V_{a2}$$

$$V_b = V_{b0} + V_{b1} + V_{b2} \quad (7)$$

$$V_c = V_{c0} + V_{c1} + V_{c2}$$

From equations (1) to (5) Zero sequence component

$$V_{a0} = V_{b0} = V_{c0}$$

Positive sequence component

$$V_{b1} = a^2 V_{a1}$$

$$V_{c1} = a V_{a1}$$

Negative sequence component

$$V_{b2} = a V_{a2}$$

$$V_{c2} = a^2 V_{a2}$$

$V_a$ ,  $V_b$  and  $V_c$  can be expressed in terms of phase "a" components only as:

$$V_a = V_{a0} + V_{a1} + V_{a2}$$

$$V_b = V_{a0} + a^2 V_{a1} + a V_{a2}$$

$$V_c = V_{a0} + a V_{a1} + a^2 V_{a2}$$

This equation can be accomplished in a matrix form:

$$\begin{bmatrix} V_a \\ V_b \\ V_c \end{bmatrix} = \begin{bmatrix} 1 & 1 & 1 \\ 1 & a^2 & a \\ 1 & a & a^2 \end{bmatrix} \begin{bmatrix} V_{a0} \\ V_{a1} \\ V_{a2} \end{bmatrix} \quad (8)$$

Equation (8) can be written as:

$$A = \begin{bmatrix} 1 & 1 & 1 \\ 1 & a^2 & a \\ 1 & a & a^2 \end{bmatrix}, \quad \begin{bmatrix} V_a \\ V_b \\ V_c \end{bmatrix} = A \begin{bmatrix} V_{a0} \\ V_{a1} \\ V_{a2} \end{bmatrix}$$

This equation can be reversed in order to obtain the positive, negative and zero sequences from the system phasors

$$\begin{bmatrix} V_{a0} \\ V_{a1} \\ V_{a2} \end{bmatrix} = A^{-1} \begin{bmatrix} V_a \\ V_b \\ V_c \end{bmatrix} \quad (9)$$

### 3.1 Symmetrical fault analysis

Three-phase fault is known the symmetrical fault where the voltage is zero in the fault site. Figure 3 shows the general simulation for the symmetrical fault, Figure 4 shows the sequence diagram of a symmetrical fault [15-16].

$$I_{a0} = 0 \quad (10)$$

$$I_{a2} = 0 \quad (11)$$

$$I_{a1} = \frac{1 \angle 0}{Z_1 + Z_f} \quad (12)$$

At fault impedance  $Z_f$  is zero,

$$I_{a1} = \frac{1 \angle 0}{Z_1}$$

Substituted into equation (13)

$$\begin{bmatrix} I_{af} \\ I_{bf} \\ I_{cf} \end{bmatrix} = \begin{bmatrix} 1 & 1 & 1 \\ 1 & a^2 & a \\ 1 & a & a^2 \end{bmatrix} \begin{bmatrix} 0 \\ I_{a1} \\ 0 \end{bmatrix} \quad (13)$$

So, by solving the equations:

Where

$$A^{-1} = \frac{1}{3} \begin{bmatrix} 1 & 1 & 1 \\ 1 & a & a^2 \\ 1 & a^2 & a \end{bmatrix}$$

$$I_{af} = \frac{1 \angle 0}{Z_1}$$

$$I_{bf} = \frac{1 \angle 240}{Z_1}$$

$$I_{cf} = \frac{1 \angle 120}{Z_1}$$

And the phase Voltage is:

$$V_{af} = V_{bf} = V_{cf} = 0 \quad (14)$$

$$V_{a0} = V_{a1} = V_{a2} = 0 \quad (15)$$

## 4. Out of Step and Distance Relaying

In this part, we will introduce the concept of power swings. It will be shown that the post fault power swings may encroach the relay characteristics. This can lead to nuisance tripping of distance relays which can sacrifice the system security.

### 4.1 Stable condition in the power system

At the steady state in the power system, the electrical loads are equalized with the mechanical torque applied to the generator. Figure 2 shows the power angle curve for the operation system that discussed in Figure 1 for the two sources. At fault in the system, the amount of the output power will reduce, but the feedback control can't increase the mechanical torque to the rotor instantaneous [17]. Figure 6 shows the stable transient point of  $\delta$  with transferring electric power  $P_0$ , this angle will change at the fault condition where the output power will reduce to PF, at this moment the generator rotor starts to accelerate the speed but the mechanical input not changed so the operation angle  $\delta$  will be increase [18]. At clearing fault, the generator angle will reach to  $\delta_c$ , because the output electrical power  $P_C$  at  $\delta_c$  is larger than the input mechanical power

P0 and the generator speed will begin to decrease, the inertia of the rotor cannot re-turn the angle  $\delta_c$  immediately to  $\delta$ . So, the angle continues to increase to  $\delta_F$ . (Area-2) is the energy lost at deceleration, its equal to the energy gained at acceleration in (Area-1) this is called equal area criterion<sup>[17,18]</sup>.

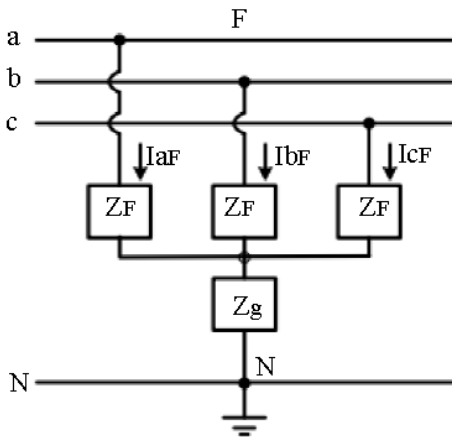


Figure 3. General simulation of a three-phase fault

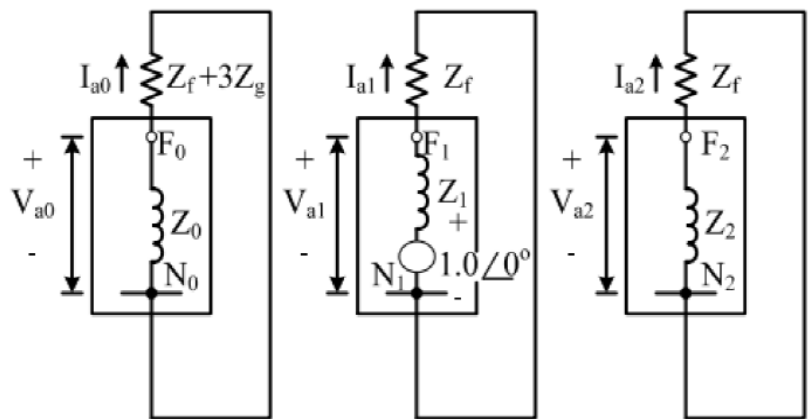


Figure 4. Sequence diagrams of a symmetrical fault

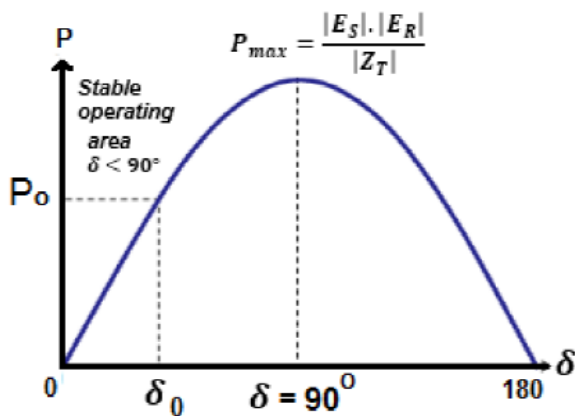


Figure 5. Power angle curve

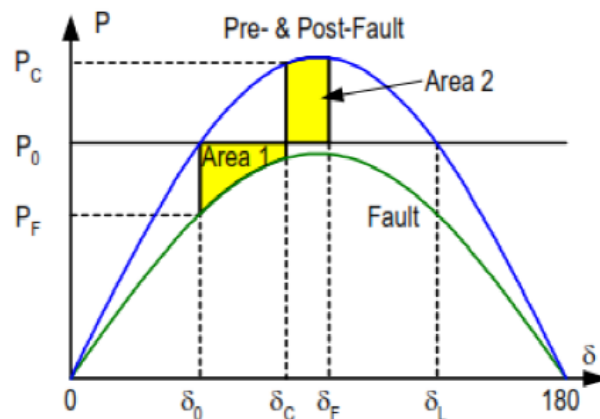


Figure 6. Steady-State transient system

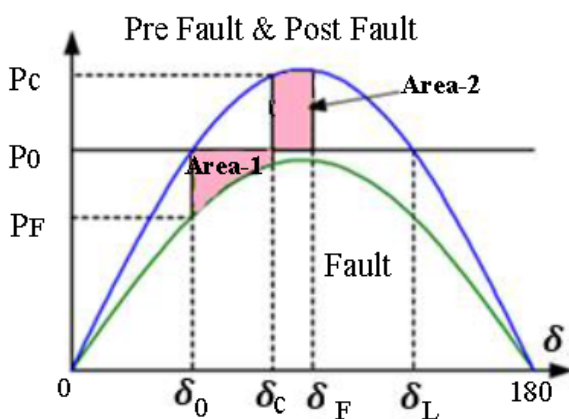


Figure 7. Unstable operation system

### 4.2 Transient unstable power system

If  $\delta_F$  is smaller than  $\delta_L$ , the system is transiently stable as shown in Figure 5, and the two sources angle difference eventually return back to original balance point  $\delta_0$ . However, if (area-2) is smaller than (area-1) the angle  $\delta$  increase to angle  $\delta_L$ . This led to the electric power output from the generators lower than the input mechanical power. Therefore, the rotor will accelerate again and  $\delta$ , it will increase beyond recovery<sup>[18]</sup>. This is a transiently unstable condition in the

system, as shown in Figure 7. At condition in the power system, the two equivalent generators rotate at a different speed leading to an unstable system. This event is called a loss of synchronism or an OOS condition in the power system [19].

### 4.3 Analysis of two area system

Power swings refer to the power flows oscillation on OHTL at the system disturbance. By consider a simple two machines system connected by a transmission line of impedance ZL as shown in Figure 1 ES and ER are the generator voltages at two ends and assume the system is purely reactive. The voltage ES leads ER by an angle  $\delta$  so that power flows from A to B during steady state. The relay under consideration is located at bus-bar-A end. The power angle curve is shown in Figure 6. The system is operating at initial steady operating point A with  $P_{m0}$  as output power and  $\delta_0$  as initial rotor angle [14-20].

From the power angle curve, initial rotor angle,

$$\delta_0 = \sin^{-1} \left( \frac{P_{m0}}{P_{max}} \right) \tag{16}$$

Now, suppose, a self-clearing transient three phase short circuit fault occurs on the line. During the fault, the electrical output power  $P_e$  drops to zero. The resulting rotor acceleration advances rotor angle to  $\delta_1$ . After a time interval  $t_{cr}$ , corresponding to angle  $\delta$ , the fault is cleared and the operating point jumps back to the sinusoidal curve. Rotor angle correspond to this instant is  $\delta_1$ . As per equal area criteria, the rotor will swing up to maximum rotor angle  $\delta_{max}$  satisfying the following condition:

Accelerating Area ( $A_1$ ) = Decelerating Area ( $A_2$ ) Rotor angle  $\delta_1$  corresponding to fault clearing time  $t_{cr}$  can be computed by swing equation [20-21].

$$\frac{2H}{\omega_s} \frac{d^2 \delta}{dt^2} = P_{m0} - P_e = P_a \tag{17}$$

where H is the equivalent rotor angle inertia.

During fault,  $P_e = 0$ , hence,

$$\frac{2H}{\omega_s} \frac{d^2 \delta}{dt^2} = P_{m0} \tag{18}$$

On integrating both the sides with respect to variable t,

$$\frac{d\delta}{dt} = \frac{\omega_s P_{m0}}{2H} (t - t_0) \tag{19}$$

Prior to fault  $\delta_0$  is a stationary point.

The initial condition of  $d\delta/dt$  is specified as follows

$$\left. \frac{d\delta}{dt} \right|_{t=t_0} = 0$$

Integrating equation (19) and substituting  $\delta = \delta_1$  at time  $t = t_1$ , with  $t_1 - t_0 = t_{cr}$ ,

$$\delta_1 = \frac{\omega_s P_{m0}}{4H} (t_{cr}^2) + \delta_0 \tag{20}$$

Thus, accelerating area  $A_1$  is given by,

$$\begin{aligned} A_1 &= \int_{\delta_0}^{\delta_1} P_{m0} d\delta = P_{m0} (\delta_1 - \delta_0) \\ &= P_{m0} (\delta_1 - \delta_0) \end{aligned} \tag{21}$$

Substituting in equation (21),

$$A_1 = \frac{\omega_s P_{m0}^2 (t_{cr}^2)}{4H} \tag{22}$$

Similarly, decelerating area, A2, can be calculated as follows.

$$A_2 = \int_{\delta_1}^{\delta_{max}} P_{max} \sin \delta d\delta = P_{max} (\cos \delta_1 - \cos \delta_{max}) - P_{m0} (\delta_{max} - \delta_1) \tag{23}$$

Since for a stable swing, A1 = A2

$$P_{m0} (\delta_1 - \delta_0) = P_{max} (\cos \delta_1 - \cos \delta_{max}) - P_{m0} (\delta_{max} - \delta_1) \tag{24}$$

$$\cos \delta_{max} = \cos \delta_1 - \frac{P_{m0}}{P_{max}} (\delta_{max} - \delta_0) \tag{25}$$

Since  $\delta_0$  is function of Pm0 from equation (16) and  $\delta_1$  is function of Pm0 as well as  $t_{cr}$  from equation (20), it follows from equation (25) that  $\delta_{max}$  depends on Pm0 and  $t_{cr}$ .

i.e.  $\delta_{max} = f(P_{m0}, t_{cr})$  (26)

The variation of  $\delta_{max}$  verses Pm0 for different values of  $t_{cr}$  is shown in Fig. 8.

#### 4.4 Determination of power swing locus

A distance relay may classify power swing as a phase fault if impedance trajectory enters the operating characteristic of the relay. We will now derive the apparent impedance seen by the relay R on R-X plane. Again, consider simple two machine system connected by a transmission line of impedance ZL as shown in Fig. 1, where machine B is treated as reference [21-22].

$$I_{relay} = \frac{E_S \angle \delta - E_R}{Z_T} \tag{27}$$

Where,  $Z_T = Z_S + Z_L + Z_R$  (28)

Now, impedance seen by relay is given by the following equation,

$$Z_{seen}(relay) = \frac{V_{relay}}{I_{relay}} = \frac{E_S \angle \delta - I_{relay} Z_S}{I_{relay}} \tag{29}$$

$$= -Z_S + Z_T \left( \frac{1}{1 - \frac{E_R}{E_S} \angle -\delta} \right)$$

$$= -Z_S + \left( \frac{E_S \angle \delta}{E_S \angle \delta - E_R} \right) Z_T$$

Let us define  $k = \left| \frac{E_S}{E_R} \right|$ .

Assuming for simplicity, both the voltages as equal to 1pu, i.e. k=1,

$$\begin{aligned}
 Z_{(relay)} &= -Z_S + Z_T \left( \frac{1}{1 - \cos \delta + j \sin \delta} \right) \\
 &= -Z_S + \frac{Z_T}{2} \left( \frac{1}{\frac{1 - \cos \delta}{2} + j \frac{\sin \delta}{2}} \right) \\
 &= -Z_S + \frac{Z_T}{2 \sin \frac{\delta}{2}} (\sin \frac{\delta}{2} - j \cos \frac{\delta}{2}) \\
 &= -Z_S + \frac{Z_T}{2} (1 - j \cot \frac{\delta}{2}) \tag{30} \\
 &= -Z_S + \frac{Z_T}{2} - j \frac{Z_T}{2} \cot \frac{\delta}{2}
 \end{aligned}$$

a constant offset      perpendicular line segment

From equation (30) at  $\delta = 180^\circ$ ,  
 $\cot \delta = 0$ ,  $Z_{seen} = -Z_S + \frac{Z_T}{2}$

There is a geometrical interpretation of above equation.

The vector component  $-Z_S + \frac{Z_T}{2}$  in equation (30) is a constant in R – X plane. The component  $-j \frac{Z_T}{2} \cot \frac{\delta}{2}$  is a straight line, perpendicular to line segment  $\frac{Z_T}{2}$ . Thus, the trajectory of the impedance measured by relay during the power swing is a straight line as shown in Figure 8. The angle subtended by a point in the locus on S and R end points is angle  $\delta$ . For simplicity, angle of  $Z_S, Z_R$  and  $Z_L$  are considered identical. It intersects the line AB at midpoint, when  $\delta = 180^\circ$ . The corresponding point of intersection of swing impedance trajectory to the impedance line is known as electrical center of the swing in Fig. 8, where, the angle  $\delta$ , between two sources can be mapped graphically as the angle subtended by source points  $E_S$  and  $E_R$  on the swing trajectory. At the electrical center, angle between two sources is  $180^\circ$ . The existence of electrical center is an indication of system instability, the two generators now being out of step [17-21].

If the power swing is stable, i.e. if the post fault system is stable, and then  $\delta_{max}$  will be less than  $180^\circ - \delta$ . In such event, the power swing retraces its path at  $\delta_{max}$ .

If  $\frac{E_S}{E_R} = k \neq 1$ , then the power swing locus on the R – X is an arc of the circle. As shown in Figure 9. It can be easily shown that

$$\frac{E_S}{E_S - E_R} = \frac{k(\cos \delta + j \sin \delta)}{k(\cos \delta + j \sin \delta) - 1} = \frac{k[(k - \cos \delta) - j \sin \delta]}{(k - \cos \delta)^2 + \sin^2 \delta} \tag{31}$$

Then,

$$Z_{seen} = -Z_S + \frac{k[(k - \cos \delta) - j \sin \delta]}{(k - \cos \delta)^2 + \sin^2 \delta} Z_T$$

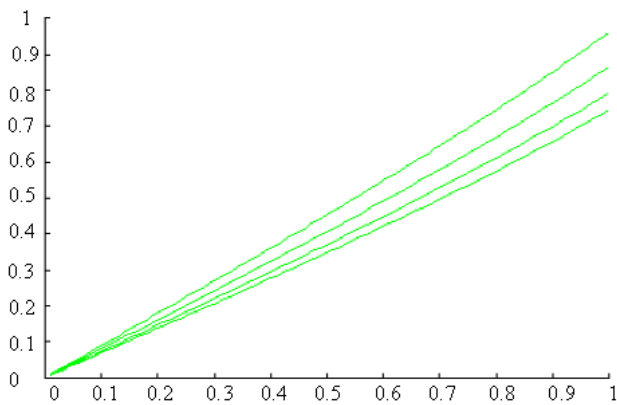


Figure 8. Plots of  $\delta_{max}$  verses  $P_{mo}$ , for different values of  $t_{cr}$

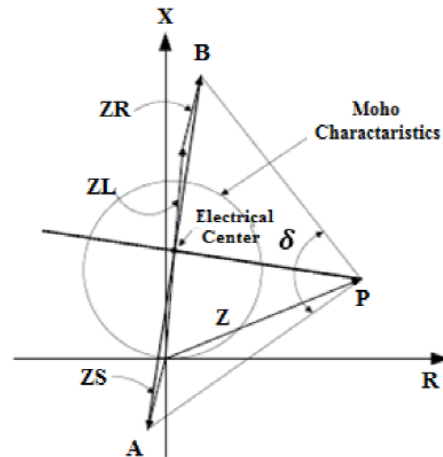


Figure 9. Intelligent relay characteristics Impedance trajectories at OOS

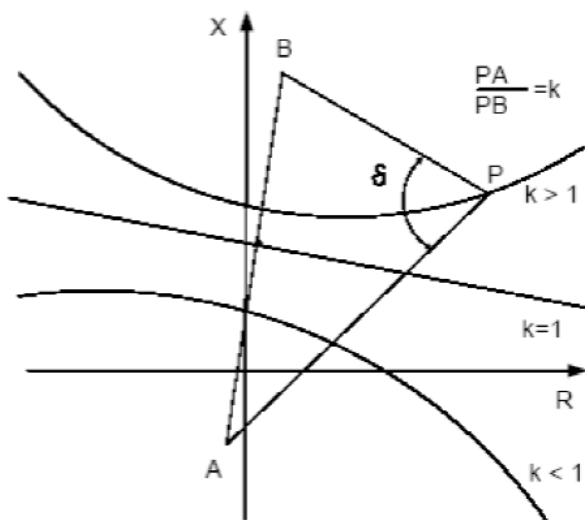


Figure 10. Impedance Trajectories at relay point during power swing

It is also clear from Figure 8 and Figure 9, that the location of the electrical center is dependent upon the  $E_s / E_r$  ratio. Appearance of electrical center on a transmission line is a transient phenomenon. The voltage profile across the transmission at the point of occurrence of electrical center is shown in Figure 10.

At the electrical center, the voltage is exactly zero. This means that relays at both the ends of line perceive it as a bolted three phase fault and immediately trip the line. Thus, we can conclude that existence of electrical center indicates (1) system instability (2) possibility of nuisance tripping of distance relay, as shown in Figure 10.

Now consider a double-end-feed transmission line with three stepped distance protection schemes having  $Z_1, Z_2$  and  $Z_3$  protection zones as shown in Figure 11 and Figure 12. The mho relays are used and characteristics are plotted on R-X plane as shown in Figure 11. Swing impedance trajectory is also overlapped on relay characteristics for a simple case of equal end voltages (i.e.  $k = 1$ ) and it is perpendicular to line AB.

From Figure 11 and Figure 12,  $\delta_{z1}, \delta_{z2}$  and  $\delta_{z3}$  are rotor angles when swing just enters the zone  $Z_1, Z_2$  and  $Z_3$  respectively and it can be obtained at the intersection of swing trajectory to the relay characteristics. Recalling  $\delta_{max}$  is the maximum rotor angle for stable power swing, following inferences can be drawn.

If  $\delta_{max} < \delta_{z3}$ , then the swing will not enter the relay characteristics.

If  $\delta z3 \leq \delta_{max} \leq \delta z2$ , the swing will enter in zone Z3. If it stays in zone - Z3 for larger interval than its TDS, then the relay will trip the line.

If  $\delta z2 \leq \delta_{max} \leq \delta z1$ , the swing will enter in both the zones Z2 and Z3. If it stays in zone 2, for larger interval than its TDS.

If  $\delta_{max} \geq \delta z1$ , the swing will enter in the zones Z1, Z2 and Z3 and operate zone 1 protection will operate without instantaneous delay.

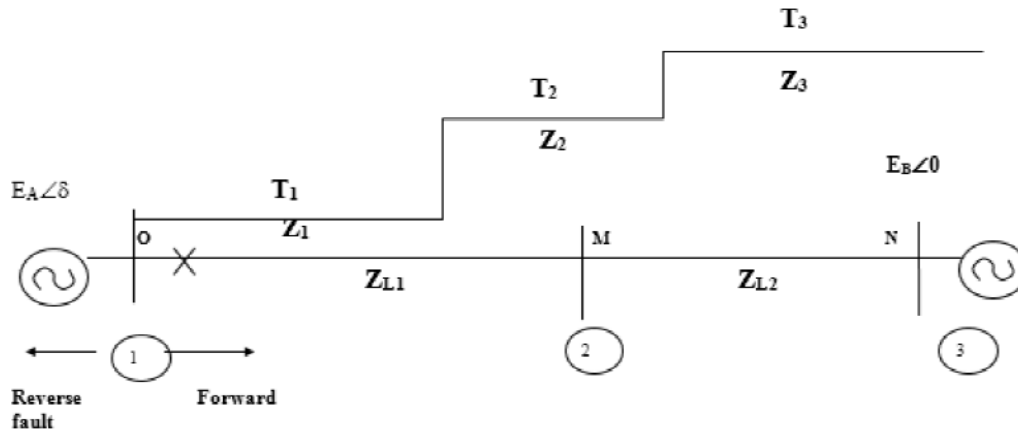


Figure 11. Single line diagram showing three protection zones

Evaluation of power swings on a multimachine system requires usage of transient stability program. Using transient stability program, post fault the relay end node voltage and line currents can be monitored and then the swing trajectory traced on impedance.

#### 4.5 OOS effect on distance function in IEDs

OOS can affect the calculations of the load impedance in IEDs, where, at steady state conditions is not within the IED operating zone characteristic, to enter the calculations into the IEDs operating zone characteristic as show in Figure 13 When impedance due to power swing matches with the operating impedance of the distance relay, it will send false tripping to the cut breaker. During OOS the IEDs may cause undesired tripping of OHTL or other power system elements, by weakening the system and possibly lead to cascading outages and the shutdown of major portions of the power system [23,24]. Figure 14 shows the three-phase current and voltage at OOS, so at the point of the voltage is low, the protection relay impedance calculation will sense this point as a fault in the system.

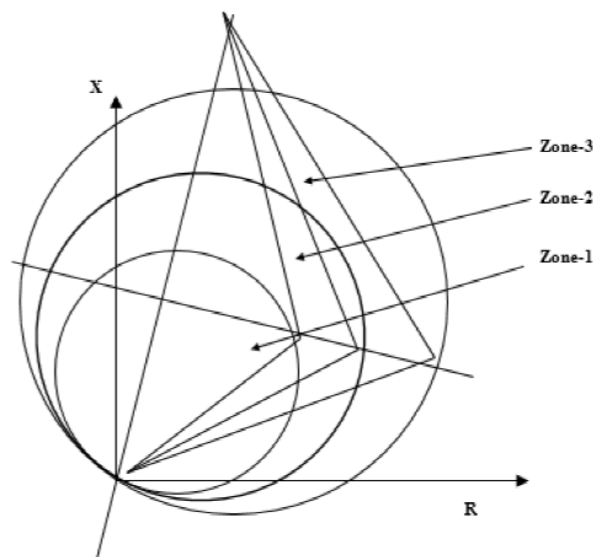


Figure 12. Three stepped distance protection

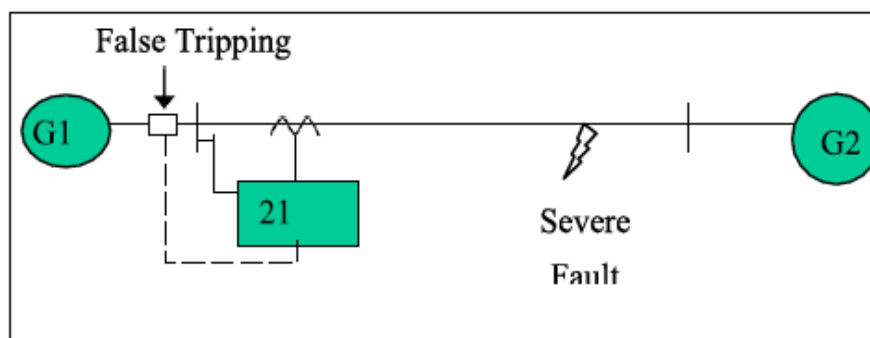


Figure 13. IED's operation logic of distance function

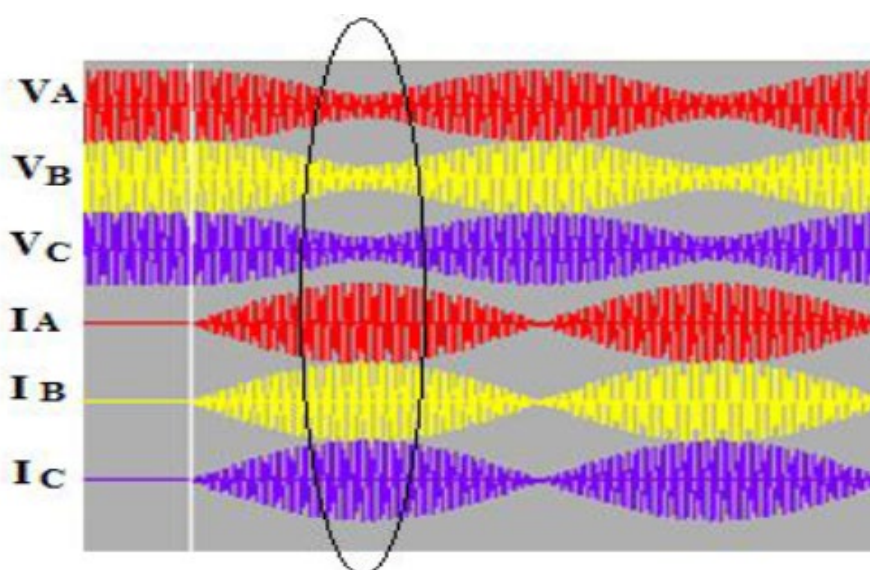


Figure 14. Voltage and current curve forms at OOS

## 5. Distance function requirements in IEDs at OOS

The operating characteristic of the distance protection is depending on the load impedance which related to voltage and current [25]. The numerical relays can adjust to sense the actual three phase fault and the OOS by the fast or gradual changing in the load impedance in the setting zone. Both faults and OOS may cause the measured apparent positive-sequence impedance to enter into the operating characteristic of a distance relay element.

In Figure 15, plot of the current and voltage over the entire 60 second at OOS. Because of the complexity and the rare occurrence of power system at OOS, many of utilities haven't clear performance that requirement for distance IEDs during OOS [26]. So, the performances of distance elements at OOS conditions must be blocking the distance function in IEDs during stable power swings in the system. But the OST function should be considered to accomplish differentiation stable from unstable power swings, and separation to system areas at the predetermined network locations and at the appropriate source-voltage phase-angle difference between systems, in order to maintain power system stability and service continuity [14-26].

### 5.1 Solution for Distance IEDs at OOS

Using the advanced protection relays which called IEDs can absorb the OOS condition in the power system. In the last parts in this paper it is discussed the difference between the three-phase symmetrical fault and the stable swing in the power system. The duration changing in the system can to analyze to three phase fault which the load impedance is decreases very fast, and the three-phase swing, the load impedance is gradually changes to inter in the distance zone setting. By creating

new logic in the IEDs to block for the symmetrical three-phase fault distance protection function [24,27]. The new logic can detect the OOS by adding new two zones greater than the bigger distance protection zone, where the stable swing will still between the two new zones for some cycle depend on the design system which can gradual change the load impedance from 3 cycles to 5 cycles [18-20]. Figure 16 shows the new creating two zones over from the actual setting for tripping three-phase fault. At the apparent load impedance still for the setting time between the outer new zone and the inner new zone, so the out of step blocking OSB element will activate to block the symmetrical three-phase fault to 2 seconds [26-28]. OST schemes require for tripping scheme to separate the power system at key locations to achieve a new steady-state operating condition. OST function will active at the unstable swing in the power system to isolate the two areas to prevent total black-out [29-32].

## 6. Experimental simulation using advanced protection relay

The experimental can to simulate in the lab by using the numerical protection relay to simulate the symmetrical three phase fault and to create the new distance function to block the distance protection function at stable swing to prevent the false operation for the three-phase distance protection.

### 6.1 Symmetrical Three-phase Simulation

Figure 17 shows the test simulation for three phase faults with IEDs which created by frejawan software to be uses with FREJA secondary injection Kit. This test applied by using a secondary injection kit type Freja300. The nominal operating voltage for this system is 132 kV. The voltage transformer ratio is 132/0.115 kV and the current transformer ratio is 1000/1 Amps, the maximum load is 1000 Amps at a  $\pm 30$ -degree power factor. The Zone 1, Zone 2, Zone 4 and distance element reaches are set to be 85 %, 130% forward direction and Zone 4 adjusted by 120 % in reverse of the line impedance, respectively. This test simulated by a protection IEDs type RED670. Table 1 shows the result point sheet for the quadrature impedance results at three phase symmetrical fault simulation.

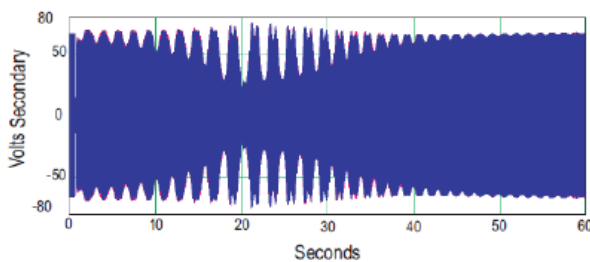


Figure 15. Voltage and current over the entire 60- second at OOS

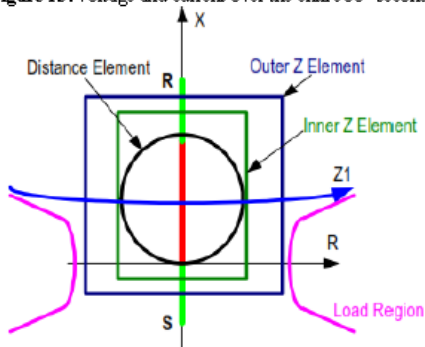


Figure 16. New quadrature outer and inner zones for out-of-step

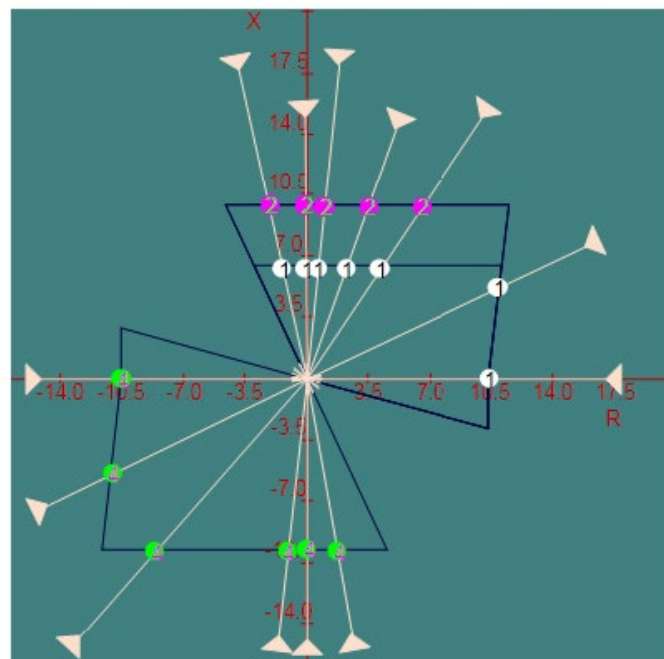


Figure 17. Triple-phase distance simulation with advanced protection relay.

Test Point	Resist. (Ω)	React. (Ω)	Impedance (Ω)	Fault angle	Tolerance Set. (%)	Result dif. (%)	Point Zone	Accept / Fail
1	10.426	0.000	10.426	0.000	10.0 %	0.3 %	1	Accept
2	0.662	6.294	6.329	84.0	10.0 %	0.2 %	1	Accept
3	1.024	9.740	9.794	84.0	8.0 %	0.7 %	2	Accept
4	0.000	6.270	6.270	90.0	10.0 %	0.4 %	1	Accept
5	0.000	9.817	9.817	90.0	8.0 %	0.2 %	2	Accept
6	-1.330	6.259	6.399	102.0	10.0 %	0.5 %	1	Accept
7	-2.084	9.805	10.024	102.0	8.0 %	0.3 %	2	Accept
8	4.186	6.252	7.524	56.2	10.0 %	0.5 %	1	Accept
9	6.553	9.789	11.780	56.2	8.0 %	0.4 %	2	Accept
10	-10.429	0.000	10.430	180.0	5.0 %	0.2 %	4	Accept
11	0.000	-9.785	9.786	270.0	5.0 %	0.4 %	4	Accept
12	1.730	-9.809	9.961	280.0	5.0 %	0.2 %	4	Accept
13	-1.035	-9.848	9.903	264.0	5.0 %	0.1 %	4	Accept
14	-8.566	-9.828	13.038	229.0	5.0 %	0.1 %	4	Accept
15	-10.967	-5.446	12.246	206.5	5.0 %	0.5 %	4	Accept
16	10.942	5.103	12.073	25.0	10.0 %	0.5 %	1	Accept
17	2.292	6.297	6.701	70.0	10.0 %	0.2 %	1	Accept
18	3.561	9.783	10.411	70.0	8.0 %	0.4 %	2	Accept

Table 1. Distance results sheet for three phase faults

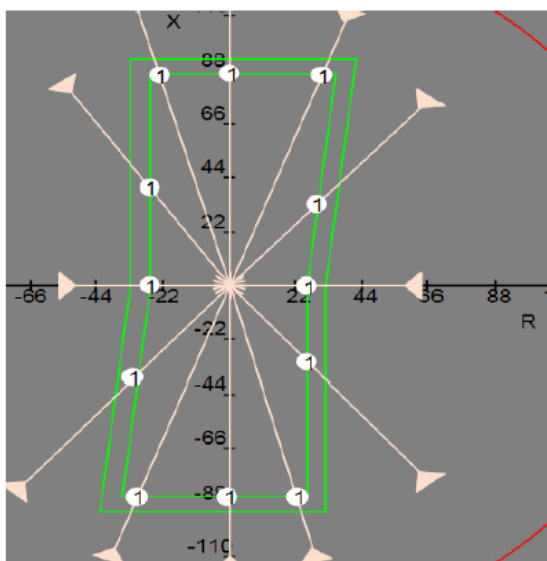


Figure 18. Test relay OOS function boundary graph for the inner zone

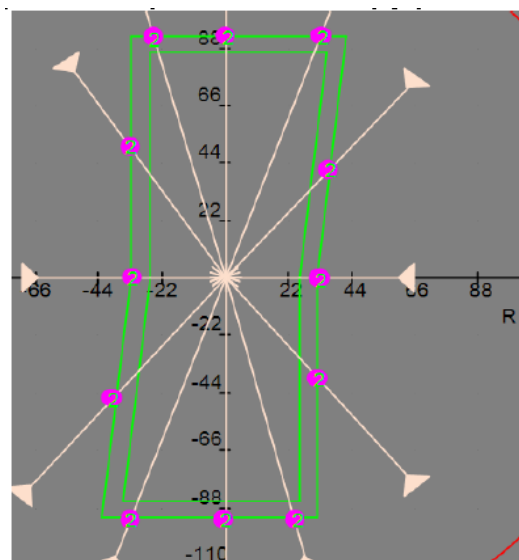


Figure 19. Test relay OOS function boundary graph for the outer zone

## 6.2 Test the boundary new zones for OOS

By using the Freja-win software can draw the new inner and outer zone that can to uses with the advanced relay to block the three-phase fault at the load impedance still in between the two new zones for 3 to 5 cycles. The secondary injection in this simulation is used the Freja 300 kit, this test applied on IEDs type RED670, this simulation for 132 kV OHTL by a maximum load of 1000A. The voltage transformer ratio is 132/0.115 kV and the current transformer ratio is 1000/1A.

Figure 18 and Figure 19 show the test results which created by the software simulation and table (2) and table (3) include report results.

## 7. Conclusion

Out-of-step (OOS) condition in the power systems can to lead to false operation for the three-phase distance relay. The OOS condition is occurred at the un-equalized between mechanical torque for the generator and the electrical loads that leads to false trip for the OHTL elements. This paper introduces an overview of OOS, their causes, and optimum method for detecting the OOS. The detecting method for OOS in the system have been developed and elaborated. This paper shows the optimum solution for the numerical protection relay for detecting the OOS, this solution easy to prevent the false trip by creating new boundary two zones over from greater tipping zone, as detecting the load symmetrical impedance between new zones for a few cycles. This will lead to blocking for the symmetrical calculating zones by the time to return the stable swing in the grid which will prevent the separating grid or system black out that improve the power system quality.

Test Point	Resist. ( $\Omega$ )	React. ( $\Omega$ )	Impedance ( $\Omega$ )	Fault angle	Tolerance Set. (%)	Result dif. (%)	Point Zone	Accept / Fail
1	31.343	86.115	91.641	70.0	5%	0.5 %	1	Accept
2	0.000	86.138	86.138	90.0	5%	0.5 %	1	Accept
3	-23.020	-85.915	88.946	105.0	5%	0.3 %	1	Accept
4	31.637	-37.703	49.219	230.0	5%	0.6 %	1	Accept
5	0.000	-85.883	85.884	270.0	5%	0.2 %	1	Accept
6	26.177	31.195	40.723	310.0	5%	0.1 %	1	Accept
7	-28.990	32.969	43.901	48.7	5%	0.8 %	1	Accept
8	-26.238	-39.833	47.698	123.4	5%	0.2 %	1	Accept
9	30.517	-86.047	91.300	250.5	5%	0.4 %	1	Accept
10	-23.001	85.839	88.868	285.0	5%	0.2 %	1	Accept
11	25.832	0.000	25.833	180.0	5%	0.4 %	1	Accept
12	25.976	0.000	25.976	0.000	5%	0.2 %	1	Accept

Table 2. Result sheet for the new design inner zone

Test Point	Resist. ( $\Omega$ )	React. ( $\Omega$ )	Impedance ( $\Omega$ )	Fault angle	Tolerance Set. (%)	Result dif. (%)	Point Zone	Accept / Fail
1	33.802	92.869	98.829	70.0	5%	0.7 %	2	Accept
2	0.000	92.540	92.540	90.0	5%	0.4 %	2	Accept
3	-24.750	-92.370	95.628	105.0	5%	0.2 %	2	Accept
4	39.019	-46.501	60.704	230.0	5%	0.5 %	2	Accept
5	0.000	-92.597	92.598	270.0	5%	0.5 %	2	Accept
6	32.579	38.825	50.684	310.0	5%	0.1 %	2	Accept
7	-36.002	40.944	54.521	48.7	5%	0.7 %	2	Accept
8	-32.759	-49.733	59.553	123.4	5%	0.3 %	2	Accept
9	32.801	-92.488	98.133	250.5	5%	0.4 %	2	Accept
10	24.805	92.571	95.838	285.0	5%	0.5 %	2	Accept
11	-33.004	0.000	33.004	0.0	5%	0.4 %	2	Accept
12	32.621	0.000	32.622	180.0	5%	0.1 %	2	Accept

Table 3. Result sheet for the new design outer zone

## References

1. Pituk Bunnoon. Fault Detection Approaches to Power System: State-of-the-Art Article Reviews for Searching a New Approach in the Future. *International Journal of Electrical and Computer Engineering (IJECE)* - 2013, p. 553-560.
2. Amer Nasr A. Elghaffar, Adel A. Elbaset: Mathematical Calculation of Electromagnetic Field in High Voltage Substation. *Annals of Faculty Engineering Journal*, 2016.
3. Yehia Sayed, Adel A. Elbaset, Amer Nasr A. Elghaffar: Treatment EMF on The Protection IEDs in HV Substations. 2017 Nineteenth International Middle East Power Systems Conference (Mepcon), Cairo-Egypt; 12/2017, DOI: 10.1109/MEPCON.2017.8301245.
4. Tolu.O. Akinbulire, Peter.O. Oluseyi, Chris. I.Esumeh. Optimal Relay Performance Using Advanced Fault Diagnostic Techniques. Department of Electrical/ Electronic Engineering University of Lagos, Akoka, Yaba, Lagos, Nigeria. *RE&PQJ*, Vol. 1, No.6, March 2008, <https://doi.org/10.24084/repqj06.393>
5. Ali M Eltamaly, Yehia Sayed, Abou-Hashema M El-Sayed, Amer Nasr A. Elghaffar: Mitigation Voltage Sag Using DVR with Power Distribution Networks for Enhancing the Power System Quality. *IJEEAS Journal*. Vol.1 No.2. Oct. 2018.
6. Ali M. Eltamaly, Amer Nasr A. Elghaffar, Yehia Sayed Mohamed, Abou-Hashema M. El-Sayed: Enhancement of Power System Quality Using PI Control Technique with DVR for Mitigation Voltage Sag. 2018 Twentieth International Middle East Power Systems Conference (MEPCON), Cairo, Egypt; 12/2018.
7. James Megger; Juan M. Gersusa. Setting and Testing of Power Swing Blocking and Out of Step Relays Considering Transient Stability Conditions. *IET 9th International Conference on Developments in Power System Protection*, 2008. DPSP. <https://doi.org/10.1049/cp:20080027>
8. Ahad Esmailian, Mladen Kezunovic. Evaluation of Fault Analysis Tool under Power Swing and Out-of-Step Conditions. 2014, North American Power Symposium (NAPS), USA, <https://doi.org/10.1109/NAPS.2014.6965415>
9. Quintin Verzosa. Realistic testing of power swing blocking and out-of-step tripping tions. 2013. 66th Annual Conference for Protective Relay Engineers, <https://doi.org/10.1109/CPRE.2013.6822056>
10. V. Anantha Lakshmi T. R. Jyothsna. Mitigation of voltage and current variations due to three phase fault in a single machine system using distributed power flow controller. 2016 International Conference on Electrical, Electronics, and Optimization Techniques (ICEEOT). India, <https://doi.org/10.1109/ICEEOT.2016.7755490>
11. Damien Tholomier, Simon Richards, Alexander Apostolov. Advanced distance protection applications for dynamic loading and out of step condition. 2007 iREP Symposium - Bulk Power System Dynamics and Control - VII. Revitalizing Operational Reliability, USA. <https://doi.org/10.1109/IREP.2007.4410560>
12. Walter A. Elmore” protective relaying theory and applications “second edition revised and expanded. 2007.
13. Swati A. Lavand and S. A. Soman. Predictive Analytic to Supervise Zone 1 of Distance Relay Using Synchrophasors. 2016, *IEEE Transactions on Power Delivery*.
14. A.P.Vaidya, Prasad A. Venikar. Distance Protection Scheme or Protection of Long Transmission Line Considering the Effect of Fault Resistance by Using the ANN Approach. *International Journal of Electrical and Electronics Engineering 2012 (IJEEE)* Vol 1, Issue 3.
15. Jorge Santam. Analysis of power systems under fault conditions. 2011, master of science, in electrical and electronic engineering at California state university, Sacramento.
16. Anubha Gupta, et al. Simultaneous fault analysis. 2014, International Conference on Power, Automation and Communication (INPAC), India, DOI: 10.1109/INPAC.2014.6981131.
17. Savu Savulescu. Real-Time Stability in Power Systems. *Power Electronics and Power System 2014 Springer Book*, doi:10.1007/978-3-319-06680-6.
18. Ramon Sandoval, et al. Dynamic simulations help improve generator protection. 2007 Power Systems Conference: Advanced Metering, Protection, Control, Communication, and Distributed Resources. <https://doi.org/10.1109/PSAMP.2007.4740896>
19. Ali M. Eltamaly, Amer Nasr Abd Elghaffar: Modeling of distance protection logic for out-of-step condition in power system. *Electrical Engineering* 11/2017. DOI:10.1007/s00202-017-0667-320.
20. Joe Mooney, P.E., Normann Fischer. Application Guidelines for Power Swing Detection on Transmission Systems. 2006, 42nd Annual Minnesota Power Systems Conference Saint Paul, Minnesota Nov. 7-9.
21. S. Gautam and S.M. Brahma. Out-of-step blocking functions in distance relay using mathematical morphology. 2012, *IET Generation, Transmission & Distribution*. <https://doi.org/10.1049/iet-gtd.2011.0514>
22. Vinaya A. Ambekar and Sanjay S. Dambhare. Comparative evaluation of out of step detection schemes for distance relays. 2012, *Power India Conference*.

23. Prashant Gawande, Pallavi Bedekar, Milind Bagewadi. An adaptive distance relay protection scheme for enhanced protection security. 2016 IEEE 6th International Conference on Power Systems (ICPS), <https://doi.org/10.1109/ICPES.2016.7584119>
24. Don Kang and Ramakrishna Gokaraju. A New Method for Blocking Third-Zone Distance Relays During Stable Power Swings. IEEE Transactions on Power Delivery (Issue: 4, Aug. 2016), IEEE-2016.
25. Ali M. Eltamaly, Amer Nasr A. Elghaffar: A Survey: HvdC System Operation and Fault Analysis. 2017, Annals Engineering Journal, Vol.4.
26. Mojdeh Abdi-Khorsand, Vijay Vittal. Modeling Protection Systems in Time-Domain Simulations: A New Method to Detect Mis-operating Relays for Unstable Power Swings. 2016, IEEE Transactions on Power Systems
27. E. F. Vaage. A solution for faults at two locations in three-phase power systems. 1940, the Bell System Technical Journal, Volume: 19, Issue: 2, P: 290 - 305
28. S. Paudyal, R. Gokaraju. Out-of-step protection for multi-machine power systems using local measurements. IEEE-2015.
29. Fang SHI. Out-of-step Prediction for Power System Using Improved Prony Algorithm. 2016, MATEC Web of Conferences 70, 10012, ICMIT.
30. Liansong Xiong, Fang Zhuo, Feng Wang. Static Synchronous Generator Model: A New Perspective to Investigate Dynamic Characteristics and Stability Issues of Grid-Tied PWM Inverter. 2016, PP: 6264 – 6280; IEEE Power Electronics Society Print
31. X. G. Magagula, D. V. Nicolae, A. A. Yusuff. The performance of distance protection relay on series compensated line under fault conditions. 2015 AF-RICON conference, <https://doi.org/10.1109/AFRCON.2015.7332035>
32. Prashant N Gawande, Sanjay S Dambhare. Novel unblocking functions for distance relay to detect symmetrical faults during power swing. 2016, Power and Energy Society General Meeting (PESGM), <https://doi.org/10.1109/PESGM.2016.7742>